

Article

Synthesis and Luminescence Properties of New Metal-Organic Frameworks Based on Zinc(II) Ions and 2,5-Thiophendicarboxylate Ligands

Anna Lysova ^{1,2}, Denis Samsonenko ^{1,2} , Danil Dybtsev ^{1,2} and Vladimir Fedin ^{1,2,*}

¹ Nikolaev Institute of Inorganic Chemistry, Siberian Branch of the Russian Academy of Sciences, 3 Lavrentieva Ave., 630090 Novosibirsk, Russia; lysova@niic.nsc.ru (A.L.); denis@niic.nsc.ru (D.S.); dan@niic.nsc.ru (D.D.)

² Department of Natural Sciences, Novosibirsk State University, 2 Pirogova Str., 630090 Novosibirsk, Russia

* Correspondence: cluster@niic.nsc.ru; Tel.: +7-383-330-94-90

Received: 29 November 2017; Accepted: 22 December 2017; Published: 24 December 2017

Abstract: Six new metal-organic frameworks based on 2,5-thiophendicarboxylate (tdc^{2-}) and zinc(II) ions were prepared in different reaction conditions, and their crystal structures were determined by XRD analysis. The compound $[\text{Zn}(\text{tdc})(\text{dabco})(\text{H}_2\text{O})]\cdot\text{DMF}$ (**1**) is based on mononuclear Zn(II) ions connected by tdc^{2-} and dabco linkers into square-grid layered nets. The compound $[\text{Zn}_3(\text{tdc})_3(\text{dabco})_2]$ (**2**) is a rare example of monocoordinated dabco ligands in the metal-organic framework chemistry. Its crystal structure contains trinuclear linear carboxylate building units, connected into a distorted primitive cubic net. Similar trinuclear units were also found in $[\text{Zn}_5(\text{tdc})_4(\text{Htdc})_2(\text{dabco})_2]\cdot 4\text{DMF}\cdot 14\text{H}_2\text{O}$ (**3**), although as a part of more complicated pentanuclear motives. The compound $[\text{Na}_2\text{Zn}(\text{tdc})_2(\text{DMF})_2]$ (**4**), quantitatively isolated by the addition of NaOH to the mixture of $\text{Zn}(\text{NO}_3)_2$ and H_2tdc , is based on 1D chain motives, interconnected by tdc^{2-} linkers into a three-dimensional framework. The compounds $[\text{Zn}_3(\text{tdc})_3(\text{DMF})_2]\cdot 0.8\text{DMF}\cdot 1.1\text{H}_2\text{O}$ (**5**) and $[\text{Zn}_3(\text{tdc})_3(\text{DMF})_3]\cdot 0.8\text{DMF}\cdot 1.3\text{H}_2\text{O}$ (**6**) were prepared in very similar reaction conditions, but with different times of heating, indirectly indicating higher thermodynamic stability of the three-dimensional metal-organic framework **6**, compared to the two-dimensional metal-organic framework **5**. The crystal structures of both **5** and **6** are based on the same trinuclear linear units as in **2**. Luminescence properties of the compounds **4–6** were studied and compared with those for Na_2tdc salt. In particular, the luminescence spectra of **4** practically coincide with those for the reference Na_2tdc , while **5** and **6** exhibit coherent shifts of peaks to higher energies. Such hypsochromic shifts are likely associated with a different effective charge on the tdc^{2-} anions in Na_2tdc and sodium-containing **4**, compared to zinc-based **5** and **6**.

Keywords: metal-organic frameworks; zinc(II) complexes; 2,5-thiophendicarboxylic acid; X-ray diffraction analysis; luminescence

1. Introduction

Porous coordination polymers (metal-organic frameworks (MOFs)) represent periodic one- (1D), two- (2D) or three-dimensional (3D) structures consisting of metal ions or polynuclear fragments connected by bridging organic ligands. For the last two decades, such compounds have been attracting a great deal of attention due to their fascinating properties and potential applications, such as luminescence sensing [1–5], storage and/or separation of a gases [6–8], heterogeneous catalysts [9–11], drug delivery [12–14], etc. To a large extent, such a variety of potential applications for MOFs is conditioned by the design of porous structures with a precise distribution of functional groups along the internal surface [15–18]. However, the rational synthesis of a target metal-organic framework is

still a very challenging task since many critical reaction parameters, such as temperature, time, solvent composition and acidity/basicity of the reaction medium [19], are hard to understand and rationalize. A systematic analysis and investigation of the reciprocal relations between synthetic conditions, on the one hand, and a crystal structure of a product, on the other, comprise a continuously topical subject of inorganic chemistry, as well as material science. In this work, six new MOFs based on zinc(II) ions and 2,5-thiophendicarboxylates (tdc^{2-}), isolated within a narrow range of reaction conditions, were obtained and characterized. The solid state photoluminescence studies suggest a ligand-centered nature of the corresponding electron transitions.

2. Materials and Methods

2.1. Reagents and Instruments

The reagents and solvents (zinc nitrate hexahydrate, ammonium oxalate monohydrate, sodium hydroxide, *N,N'*-dimethylformamide (DMF) (all from "Reactiv", Novosibirsk, Russia), acetonitrile (MeCN) ("Cryochrom", St. Petersburg, Russia), 2,5-thiophendicarboxylic acid (H_2tdc , "TCI", Tokyo, Japan), 1,4-diazobicyclo[2,2,2]octane (dabco), triethylamine (NMe_3), ethylene glycol (all from "Sigma-Aldrich", St. Louis, MI, USA) were at least of reagent grade and used as purchased without additional purification. FT-IR spectra were recorded in the range 400–4000 cm^{-1} for the KBr-pelleted samples on a VERTEX 80 spectrometer ("Bruker", Billerica, MO, USA). The elemental analyses were obtained on an analyzer Vario MICRO Cube ("Elementar Analysensysteme", Langenselbold, Germany). The powder X-ray diffraction data were obtained on a Shimadzu XRD 7000S powder diffractometer (Cu-K α irradiation, "Shimadzu", Duisburg, Germany). The thermogravimetric analyses were carried out in He or O_2/Ar atmosphere on a NETZSCH TG 209 F1 thermoanalyzer ("NETZSCH", Selb, Germany) with the heating rate of 10 deg/min. The luminescence spectra were recorded on a FluoroLog@-3 Photoluminescence Spectrometer (Horiba Jobin Yvon S.A.S., Villeneuve d'Ascq, France), equipped by a 450-W xenon lamp, an excitation/emission monochromator and an FL-1073 PMT detector. The excitation was performed with $\lambda_{\text{ex}} = 350$ nm, and the emission was recorded at $\lambda_{\text{em}} = 425$ nm. Quantum yield was measured using an integrating sphere.

2.2. Single-Crystal X-ray Diffraction

The diffraction data for the compounds 1–6 were collected on an automated Agilent Xcalibur diffractometer (Agilent Technologies, Santa Clara, CA, USA) equipped with a two-dimensional AtlasS2 detector (graphite monochromator, $\lambda(\text{MoK}\alpha) = 0.71073$ Å, ω -scans). Integration, absorption correction and determination of unit cell parameters were performed using the CrysAlisPro program package [20]. The structures were solved by a dual space algorithm (SHELXT [21]) and refined by the full-matrix least squares technique (SHELXL [22]) in the anisotropic approximation (except hydrogen atoms). Positions of hydrogen atoms of organic ligands were calculated geometrically and refined in the riding model. In all structures, solvate guest molecules are highly disordered and could not be modeled as a set of discrete atomic sites. The final formula of the compound 3 was calculated from the data of the PLATON/SQUEEZE procedure [23] (1191 \bar{e} in 4359 Å³). The crystallographic data and details of the structure refinements are summarized in Table 1. Selected interatomic distances and valence angles are given in Tables S1–S6. CCDC 1586559–1586564 contain the supplementary crystallographic data for this paper. These data can be obtained free of charge from The Cambridge Crystallographic Data Center at http://www.ccdc.cam.ac.uk/data_request/cif.

Table 1. Crystal data and structure refinement for 1–6, 130 K.

Compound	1	2	3	4	5	6
CCDC deposition number	1586559	1586560	1586561	1586562	1586563	1586564
Empirical formula	C ₁₅ H ₂₃ N ₃ O ₆ SZn	C ₃₀ H ₃₀ N ₄ O ₁₂ S ₃ Zn ₃	C ₆₀ H ₉₄ N ₈ O ₄₂ S ₆ Zn ₅	C ₁₈ H ₁₈ N ₂ Na ₂ O ₁₀ S ₂ Zn	C ₂₆ H ₂₃ N ₃ O ₁₄ S ₃ Zn ₃	C ₂₇ H ₂₇ N ₃ O ₁₅ S ₃ Zn ₃
<i>M</i> , g/mol	438.79	930.87	2128.16	597.81	893.76	925.80
Crystal system	Orthorhombic	Monoclinic	Monoclinic	Orthorhombic	Monoclinic	Monoclinic
Space group	<i>Cmm2</i>	<i>P2₁/c</i>	<i>C2/c</i>	<i>Ama2</i>	<i>P2₁/n</i>	<i>P2₁/c</i>
<i>a</i> , Å	20.7976(8)	10.3232(4)	26.8663(7)	21.4918(6)	16.8119(5)	17.7558(4)
<i>b</i> , Å	14.0097(6)	17.9750(4)	19.2844(4)	18.8280(5)	9.6409(2)	9.7309(2)
<i>c</i> , Å	6.0284(2)	10.5364(4)	18.3894(4)	5.76625(15)	21.1725(6)	21.0282(5)
β, deg.	90	113.613(4)	99.832(2)	90	108.925(3)	103.575(2)
<i>V</i> , Å ³	1756.48(12)	1791.43(12)	9387.6(4)	2333.30(11)	3246.17(16)	3531.75(14)
<i>Z</i>	4	2	4	4	4	4
<i>D</i> (calc.), g/cm ³	1.659	1.726	1.506	1.702	1.829	1.741
μ, mm ^{−1}	1.556	2.234	1.481	1.327	2.465	2.271
<i>F</i> (000)	912	944	4388	1216	1800	1872
Crystal size, mm	0.48 × 0.09 × 0.03	0.29 × 0.08 × 0.03	0.28 × 0.26 × 0.14	0.45 × 0.15 × 0.05	0.17 × 0.15 × 0.05	0.25 × 0.21 × 0.09
θ range for data collection, deg.	3.28–28.83	3.74–29.66	3.41–29.56	3.57–29.10	3.32–29.56	3.42–29.01
Index ranges	−28 ≤ <i>h</i> ≤ 20, −19 ≤ <i>k</i> ≤ 17, −7 ≤ <i>l</i> ≤ 7	−10 ≤ <i>h</i> ≤ 14, −24 ≤ <i>k</i> ≤ 17, −13 ≤ <i>l</i> ≤ 13	−25 ≤ <i>h</i> ≤ 34, −26 ≤ <i>k</i> ≤ 19, −25 ≤ <i>l</i> ≤ 22	−28 ≤ <i>h</i> ≤ 24, −16 ≤ <i>k</i> ≤ 23, −6 ≤ <i>l</i> ≤ 7	−22 ≤ <i>h</i> ≤ 16, −13 ≤ <i>k</i> ≤ 12, −21 ≤ <i>l</i> ≤ 29	−23 ≤ <i>h</i> ≤ 23, −10 ≤ <i>k</i> ≤ 12, −28 ≤ <i>l</i> ≤ 23
Reflections collected / independent	3486 / 1797	9004 / 4233	26598 / 11162	4891 / 2302	17138 / 7667	17555 / 7800
<i>R</i> _{int}	0.0185	0.0193	0.0260	0.0178	0.0242	0.0238
Reflections with <i>I</i> > 2σ(<i>I</i>)	1713	3491	9856	2291	6469	6807
Goodness-of-fit on <i>F</i> ²	1.031	1.054	1.089	1.276	1.038	1.031
Final <i>R</i> indices [<i>I</i> > 2σ(<i>I</i>)]	<i>R</i> ₁ = 0.0233, <i>wR</i> ₂ = 0.0576	<i>R</i> ₁ = 0.0450, <i>wR</i> ₂ = 0.1045	<i>R</i> ₁ = 0.0391, <i>wR</i> ₂ = 0.0977	<i>R</i> ₁ = 0.0582, <i>wR</i> ₂ = 0.1593	<i>R</i> ₁ = 0.0271, <i>wR</i> ₂ = 0.0584	<i>R</i> ₁ = 0.0271, <i>wR</i> ₂ = 0.0599
<i>R</i> indices (all data)	<i>R</i> ₁ = 0.0251, <i>wR</i> ₂ = 0.0584	<i>R</i> ₁ = 0.0578, <i>wR</i> ₂ = 0.1117	<i>R</i> ₁ = 0.0454, <i>wR</i> ₂ = 0.1008	<i>R</i> ₁ = 0.0584, <i>wR</i> ₂ = 0.1594	<i>R</i> ₁ = 0.0371, <i>wR</i> ₂ = 0.0620	<i>R</i> ₁ = 0.0343, <i>wR</i> ₂ = 0.0630
Largest diff. peak / hole, e/Å ³	0.336 / −0.286	1.161 / −0.732	0.820 / −0.638	0.874 / −1.437	0.544 / −0.376	0.525 / −0.402

2.3. Synthetic Procedures and Analyses

2.3.1. Synthesis of $[\text{Zn}(\text{tdc})(\text{dabco})(\text{H}_2\text{O})]\cdot\text{DMF}$ (1)

Zero-point-one-six grams (0.54 mmol) $\text{Zn}(\text{NO}_3)_2\cdot 6\text{H}_2\text{O}$, 0.046 g (0.27 mmol) H_2tdc , 0.015 g (0.13 mmol) dabco and 0.038 g (0.27 mmol) ammonium oxalate monohydrate in 3.2 mL DMF were stirred with a magnetic stirrer for 1 h. An opaque solution was filtered, and NMe_3 (9.3 μL , 0.067 mmol) was added to the supernatant. The mixture was homogenized in an ultrasonic bath and filtered again. The vial with the resulting supernatant solution was heated at 130 °C for 2 days. The product **1** was isolated as colorless plate single-crystals, whose crystal structure and chemical composition were established by a single-crystal X-ray diffraction method.

2.3.2. Synthesis of $[\text{Zn}_3(\text{tdc})_3(\text{dabco})_2]$ (2)

Zero-point-zero-eight grams (0.27 mmol) $\text{Zn}(\text{NO}_3)_2\cdot 6\text{H}_2\text{O}$, 0.046 g (0.27 mmol) H_2tdc and 0.015 g (0.13 mmol) dabco in 2.0 mL DMF and 0.5 mL MeCN were stirred with a magnetic stirrer for 1 h. Then, 0.7 mL of ethylene glycol were added; the vial was closed and kept at 130 °C for 2 days. Some single crystals in the form of plates were isolated, and their crystal structure and chemical composition were established by a single-crystal X-ray diffraction method.

2.3.3. Synthesis of $[\text{Zn}_5(\text{tdc})_4(\text{Htdc})_2(\text{dabco})_2]\cdot 4\text{DMF}\cdot 14\text{H}_2\text{O}$ (3)

Zero-point-zero-two grams (0.07 mmol) $\text{Zn}(\text{NO}_3)_2\cdot 6\text{H}_2\text{O}$, 0.013 g (0.07 mmol) H_2tdc and 0.002 g (0.02 mmol) dabco in 1.4 mL DMF and 0.7 mL MeCN were stirred with a magnetic stirrer for 1 h. Then, 1.1 mL of ethylene glycol were added; the vial was closed and kept at 70 °C for 13 days. Some single thick rhombohedral plates were isolated (0.003 g, 2%), and their crystal structure and chemical composition were established by a single-crystal X-ray diffraction method and confirmed by an elemental analysis.

Elemental analyses. Found: C 34.3, H 4.4, N 5.6, S 9.0%. Calculated for $[\text{Zn}_5(\text{tdc})_4(\text{Htdc})_2(\text{dabco})_2]\cdot 4\text{DMF}\cdot 14\text{H}_2\text{O}$: C 34.0, H 4.5, N 5.3, S 9.1%.

2.3.4. Synthesis of $[\text{Na}_2\text{Zn}(\text{tdc})_2(\text{DMF})_2]$ (4)

A microcrystalline powder of the compound **4** formed in the reaction of 0.08 g (0.27 mmol) $\text{Zn}(\text{NO}_3)_2\cdot 6\text{H}_2\text{O}$, 0.093 g (0.54 mmol) H_2tdc and 0.022 g (0.54 mmol) NaOH in 3.2 mL DMF. The mixture was sonicated till a homogeneous suspension was formed, which was sealed in a vial and heated at 130 °C for 3 h. A microcrystalline powder was filtered, washed by DMF and dried in air. Yield: 0.16 g (ca. 99%). Elemental analyses: Found: C 36.0, H 3.0, N 4.7, S 11.4%. Calculated for $[\text{Na}_2\text{Zn}(\text{tdc})_2(\text{DMF})_2]$: C 36.2, H 3.0, N 4.7, S 10.7%. TG analysis. Found (wt% loss): 6% at 70 °C, 23% at 280 °C. Calculated for 2 H_2O : 6%, 2DMF: 23%. IR data (cm^{-1}): 3862 (w), 3606 (w), 3347 (w), 3177 (w), 3101 (m), 3091 (w), 3058 (w), 2994 (w), 2953 (m), 2932 (m), 2863 (m), 2804 (w), 2788 (w), 2767 (m), 2582 (w), 2014 (w), 1833 (w), 1672 (s), 1592 (s), 1543 (w), 1533 (m), 1495 (w), 1469 (w), 1437 (w), 1385 (w), 1364 (s), 1342 (w), 1320 (w), 1252 (w), 1135 (m), 1096 (c), 1064 (w), 1036 (s), 924 (w), 848 (m), 810 (s), 774 (s), 685 (m), 662 (m), 572 (w), 5581 (w), 545 (w), 508 (m), 478 (w), 406 (w) (Figure S1).

The needle-like crystals of **4**, suitable for single-crystal XRD, could be obtained in a slightly modified procedure. The above-mentioned homogeneous suspension was filtered, and a supernatant solution was heated in a sealed vial at 130 °C for 1 day. The needle-like crystals of **4** were isolated (0.02 g, 13%).

The compound **4** can be also obtained, although with notably lower yields not exceeding 60%, when other sodium(I) salts (NaNO_3 , NaClO_4 , NaCl, NaBr) are added to the reaction mixture instead of NaOH.

2.3.5. Synthesis of $[\text{Zn}_3(\text{tdc})_3(\text{DMF})_2] \cdot 0.8\text{DMF} \cdot 1.1\text{H}_2\text{O}$ (**5**)

Zero-point-zero-six grams (0.20 mmol) $\text{Zn}(\text{NO}_3)_2 \cdot 6\text{H}_2\text{O}$ and 0.034 g (0.20 mmol) H_2tdc in 3.2 mL DMF/MeCN mixture (1:1 by volume) were stirred with a magnetic stirrer for 1 h, followed by heating at 90 °C for 1 day in a sealed glass vial. The crystals in the form of rectangular plates with skew edges were filtered, washed by DMF and dried in air. Yield: 0.033 g (53%). Elemental analyses: Found: C 34.15, H 2.7, N 4.0, S 10.2%. Calculated for $[\text{Zn}_3(\text{tdc})_3(\text{dmf})_2] \cdot 0.8\text{DMF} \cdot 1.1\text{H}_2\text{O}$: C 34.06, H 3.0, N 4.2, S 10.3%. TG analysis. Found (wt% loss): 6% at 165 °C, 16% at 265 °C. Calculated for 0.8 DMF: 6%, 2DMF: 16%. IR data (cm^{-1}): 3398 (w), 3266 (w), 3111 (w), 2932 (w), 1670 (s), 1647 (w), 1622 (w), 1597 (w), 1575 (m), 1559 (s), 1532 (m), 1471 (w), 1383 (s), 1372 (s), 1309 (w), 1253 (w), 1204 (w), 1110 (m), 1064 (w), 1044 (w), 1024 (w), 841 (w), 823 (w), 811 (w), 767 (s), 682 (m), 572 (w), 522 (w), 500 (w), 466 (m), 379 (w) (Figure S2).

2.3.6. Synthesis of $[\text{Zn}_3(\text{tdc})_3(\text{DMF})_3] \cdot 0.8\text{DMF} \cdot 1.3\text{H}_2\text{O}$ (**6**)

The synthesis of **6** was carried out in an exactly the same conditions as for **5**, but the resulting reaction mixture was heated at 90 °C for 2 days. The polyhedral crystals were filtered, washed by DMF and dried in air. Yield: 0.038 g (58%). Elemental analyses: Found: C 35.15, H 3.2, N 5.2, S 9.3%. Calculated for $[\text{Zn}_3(\text{tdc})_3(\text{dmf})_3] \cdot 0.8\text{DMF} \cdot 1.3\text{H}_2\text{O}$: C 35.04, H 3.5, N 5.3, S 9.5%. TG analysis. Found (wt% loss): 22% at 260 °C. Calculated for 3DMF: 22%. IR data (cm^{-1}): 3420 (w), 3113 (w), 2932 (m), 2817 (w), 2582 (w), 1668 (m), 1576 (m), 1528 (w), 1372 (s), 1252 (w), 1110 (s), 1048 (w), 1024 (w), 823 (m), 779 (w), 766 (s), 683 (s), 558 (w), 500 (w), 464 (w) (Figure S3).

3. Results

The colorless plane single crystals $[\text{Zn}(\text{tdc})(\text{dabco})(\text{H}_2\text{O})] \cdot \text{DMF}$ (**1**, DMF = *N,N'*-dimethylformamide) were manually isolated out of the reaction mixture of $\text{Zn}(\text{NO}_3)_2$, 2,5-thiophenedicarboxylic acid (H_2tdc), 1,4-diazobicyclo[2,2,2]octane (dabco) and $(\text{NH}_4)_2(\text{C}_2\text{O}_4)$ in DMF solvent. The crystal structure and chemical composition of **1** were established by the single-crystal X-ray diffraction method. The asymmetric unit of **1** contains a zinc(II) cation, the coordination environment of which consists of two N atoms of two dabco ligands and four O atoms of two carboxylate groups of two tdc^{2-} anions and an aqua-ligand (Figure S4). Zn–O distances are in the range 2.016(3)–2.328(4) Å, and the Zn–N distance is 2.202(2) Å. One of the COO-groups is coordinated to zinc bidentately with one Zn–O distance being longer than another one. Each tdc^{2-} anion connects with two Zn(II) cations to form a polymeric carboxylate chain. Polymeric chains connect with each other via bridging dabco ligands with the formation of metal-organic layers with a square-grid topology (**sql**), parallel to the *ab* plain (Figure 1). Such grids are packed one atop another (AAAA packing mode), forming open channels in the *c* crystallographic direction with a rectangular cross-section, which are filled with guest DMF molecules.

The colorless plate single crystals $[\text{Zn}_3(\text{tdc})_3(\text{dabco})_2]$ (**2**) were manually isolated out of the reaction mixture of $\text{Zn}(\text{NO}_3)_2$, H_2tdc and dabco in the DMF/acetonitrile/ethylene glycol mixture. The crystal structure and chemical composition of **2** were established by the single-crystal X-ray diffraction method. The asymmetric unit in **2** contains two zinc(II) cations. Zn(1) is located in a distorted octahedral coordination environment of six O atoms of six tdc^{2-} anions. Zn(2) has a distorted tetrahedral coordination environment, which consists of three O atoms of three tdc^{2-} anions and one N atom of a terminal dabco ligand (Figure S5). The Zn–O distances are in the range 1.919(3)–2.117(5) Å, and the Zn–N distance is 2.049(3) Å. Zn(1) connects two Zn(2) via six bridging COO-groups to form a trinuclear unit $\{\text{Zn}_3(\mu_2\text{-RCOO})_6(\text{dabco})_2\}$ (Figure 2a), which in turn, are connected to each other via bridging tdc^{2-} anions to form a 3D MOF (Figure 2b) with primitive-cubic topology (**pcu**).

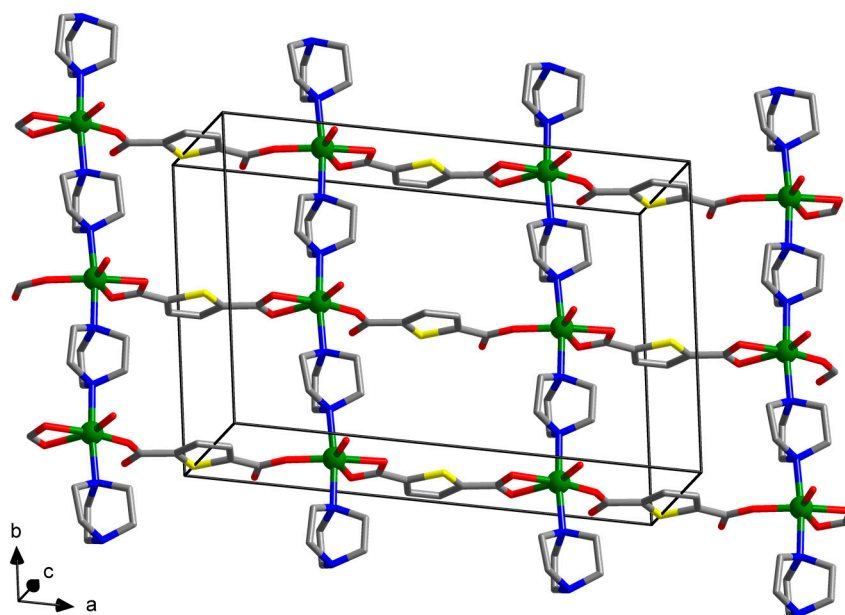


Figure 1. Fragment of the polymeric layer in the structure 1. Hydrogen atoms are omitted. Zn(II) cations are shown with green balls.

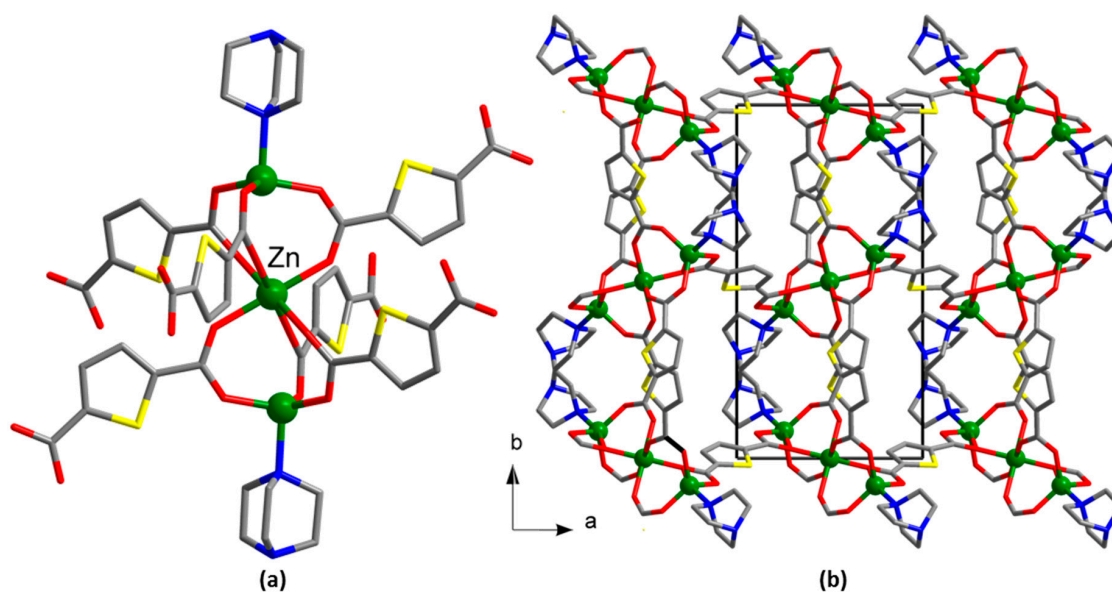


Figure 2. (a) Structure of a three-nuclear unit in the structure 2; (b) crystal packing in the structure 2. Hydrogen atoms are omitted. Only one of the possible orientations of tdc^{2-} ligands is shown. Zn(II) cations are shown with green balls.

The compound $[\text{Zn}_5(\text{tdc})_4(\text{Htdc})_2(\text{dabco})_2] \cdot 4\text{DMF} \cdot 14\text{H}_2\text{O}$ (**3**) was prepared by heating of $\text{Zn}(\text{NO}_3)_2$, H_2tdc and dabco in a DMF/acetonitrile/ethylene glycol mixture. The product was isolated as colorless thick rhombohedral plate single crystals with low yield, allowing the characterization of the compound by XRD and microelemental analyses only. The asymmetric unit of the structure **3** contains three Zn(II) cations. One Zn(1) and two Zn(2) cations connect each other via six bridging COO-groups of tdc^{2-} anions to form trinuclear unit $\{\text{Zn}_3(\mu_2\text{-RCOO})_6(\text{dabco})_2\}$ similar to that found in the structure **2**. The Zn(3) cation has a distorted tetrahedral coordination environment consisting of three O atoms of three tdc^{2-} anions and one N atom of dabco ligand to form the tetrahedral $\{\text{Zn}(\text{RCOO})_3\}$ coordination node (Figure S6). Zn–O distances are in the range 1.9298(17)–2.1033(17)

Å, and Zn–N distances are 2.061(2) and 2.098(2) Å. Each $\{Zn_3(\mu_2\text{-RCOO})_6(\text{dabco})_2\}$ unit connects two mononuclear $\{Zn(\text{RCOO})_3\}$ fragments via bridging dabco ligands to form complex pentanuclear blocks $\{Zn_5(\mu_2\text{-RCOO})_6(\text{dabco})_2(\text{RCOO})_6\}$ (Figure 3a). These blocks are interconnected via bridging tdc^{2-} anions to form a 3D open metal-organic framework (Figure 3b) with complicated topology and high accessible void volume (46% by PLATON). The pores consist of two types of intersecting channels running along the *b* and *c* axes, respectively (Figure S7), filled with highly disordered solvent DMF and water molecules, whose composition was established by the PLATON SQUEEZE routine and microelemental analysis.

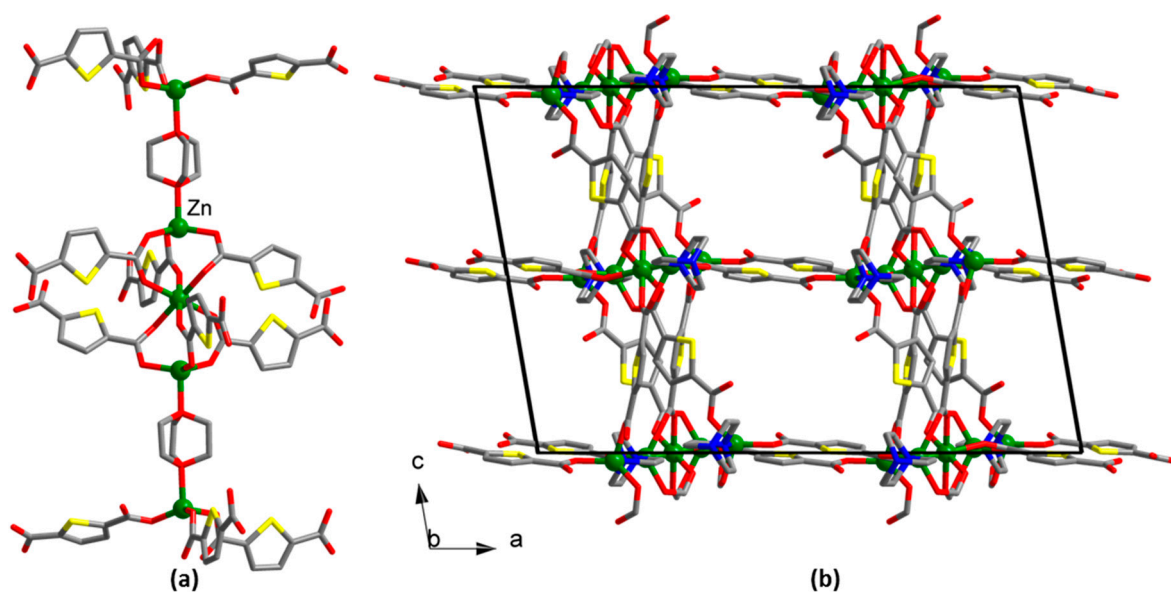


Figure 3. (a) Structure of a five-nuclear unit in the structure 3; (b) crystal packing of the structure 3. Hydrogen atoms are omitted. Only one of the possible orientations of tdc^{2-} ligands is shown. Zn(II) cations are shown with green balls.

The compound $[\text{Na}_2\text{Zn}(\text{tdc})_2(\text{DMF})_2]$ (**4**) was obtained with almost quantitative yield by heating of $\text{Zn}(\text{NO}_3)_2$, H_2tdc and NaOH in DMF solvent. Its crystal structure and chemical composition were established by a single-crystal X-ray diffraction method and confirmed by elemental, thermogravimetric analyses and IR data. An asymmetric unit of the structure 4 contains one Zn(II) cation and one Na(I) cation (Figure S8). The Na^+ cation has a distorted octahedral coordination environment consisting six O atoms of one DMF molecule and five coordinated COO-groups. The Na–O distances are in the range 2.243(3)–2.647(2) Å. The Zn(II) cation also has a distorted octahedral coordination environment, which consists of six O atoms of five COO-groups. One of the COO-groups is coordinated to zinc bidentately with one Zn–O distance being longer than the other one. The Zn–O distances are in the range 1.981(4)–2.422(5) Å. Zn(II) and Na(I) cations are interconnected via bridging COO-groups to form polymeric carboxylate chains running along the *c* axis (Figure 4a). The chains are interconnected via bridging tdc^{2-} anions along the *a* and *b* directions to form a 3D metal-organic framework (Figure 4b).

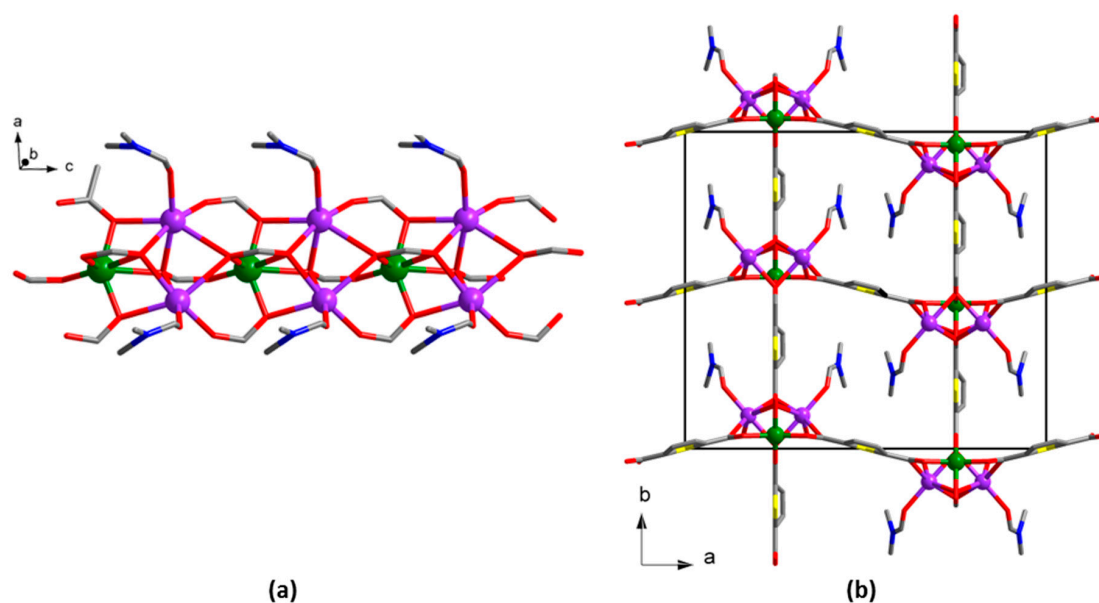


Figure 4. (a) Fragment of a polymeric chain in the structure 4; (b) crystal packing of the structure 4. Hydrogen atoms are omitted. Only one of the possible orientations of tdc²⁻ ligands and DMF molecules is shown. Zn(II) cations are shown with green balls, and Na⁺ cations are shown with violet balls.

The powder X-ray diffraction data clearly support the phase purity of the sample (Figure 5). Microelemental (Carbon-Hydrogen-Nitrogen-Sulfur, CHNS) analyses, thermogravimetric analysis and FT-IR spectroscopy confirm the chemical formula of 4 and support the nature of the compound. The TGA of 4 shows a three-step decomposition curve (Figure S9). The first weight loss (6.0 mass. %) at 70 °C corresponds to two H₂O molecules. The second step (23%) at 280 °C corresponds to the evaporation of two coordinated DMF molecules. The irreversible decomposition of the framework 4 takes place above 300 °C. The IR spectrum of 4 shows typical stretchings for carboxylate groups (1592 and 1364 cm⁻¹), C–H valence vibrations (3101–2863 cm⁻¹) and the characteristic peak for the C=O group of the DMF molecules (1672 cm⁻¹) (Figure S1). Photoluminescence measurements of 4 reveal a broad excitation peak at $\lambda = 375$ nm (detection at 425 nm) and a broad emission peak at $\lambda = 434$ nm (excitation at 350 nm).

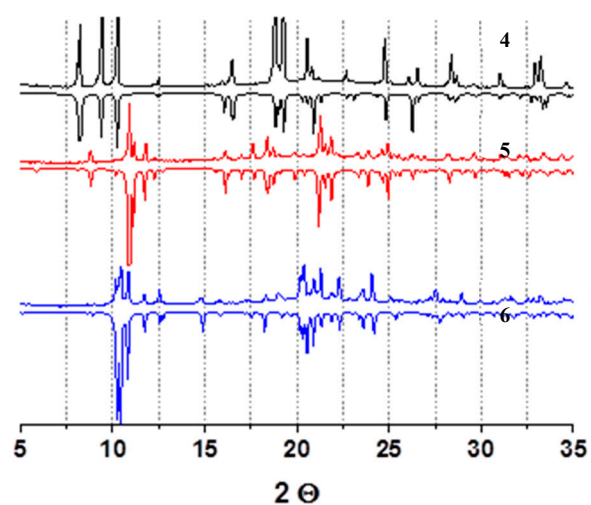


Figure 5. Powder X-ray diffraction data for compounds 4 (black), 5 (red) and 6 (blue). The experimental data (normal graphs) were collected at room temperature. The theoretical plots (reverse graphs) are simulated from the corresponding single-crystal X-ray diffraction data, collected at 130 K.

The compound $[\text{Zn}_3(\text{tdc})_3(\text{DMF})_2] \cdot 0.8\text{DMF} \cdot 1.1\text{H}_2\text{O}$ (**5**) was prepared by solvothermal reaction of $\text{Zn}(\text{NO}_3)_2$ and H_2tdc in a DMF/acetonitrile mixture at 90°C . After one day, the product was isolated as colorless rectangular plate single crystals (Figure S10a), the structure and chemical composition of which were established by a single-crystal X-ray diffraction method and confirmed by elemental, thermogravimetric and IR analysis. The asymmetric unit of **5** contains three Zn(II) cations. Zn(1) and Zn(3) have distorted tetrahedral coordination environment consisting of four O atoms of three tdc^{2-} anions and a DMF ligand (Figure S10). Zn(2) has a distorted octahedral coordination environment of six O atoms of six tdc^{2-} anions. Zn–O distances are in the range 1.9223(15)–2.1911(15) Å. Zn(II) cations are interconnected via bridging COO-groups to form trinuclear unit $\{\text{Zn}_3(\mu_2\text{-RCOO})_6\}$ (Figure 6a). Such units are interconnected via bridging tdc^{2-} anions to form trigonal metal-organic layers (**hxl**) running parallel to the *ab* plane (Figure 6b).

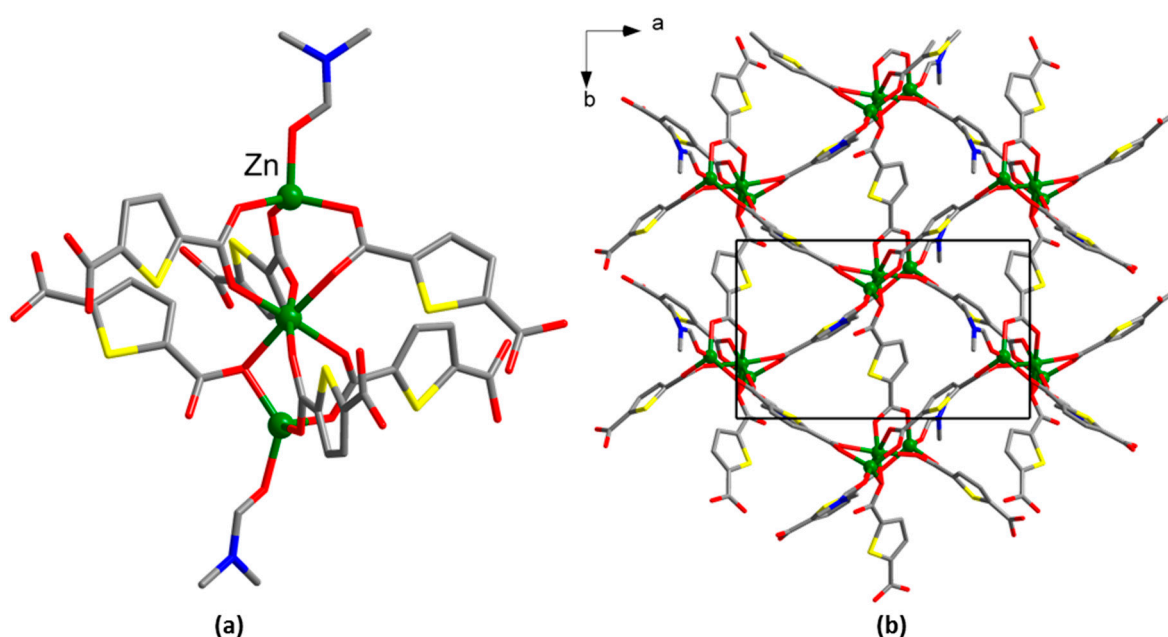


Figure 6. (a) Structure of a three-nuclear unit in the structure **5**; (b) fragment of the polymeric layer in the structure **5**. Hydrogen atoms are omitted. Zn(II) cations are shown with green balls.

The powder X-ray diffraction data support the phase purity of the bulk sample (Figure 5). Microelemental (CHNS) analyses, thermogravimetric analysis and FT-IR spectroscopy confirm the chemical formula of **5** and support the nature of the compound. The TGA of **5** shows a three-step decomposition curve (Figure S11). The first weight loss (6.0 mass. %) at 165°C corresponds to 0.8 DMF molecules. The second step (16%) at 265°C corresponds to the evaporation of two coordinated DMF molecules. The irreversible decomposition of the framework **5** takes place above 320°C . The IR spectrum of **5** shows typical stretchings for carboxylate groups (1559 and 1383 cm^{-1}), C–H valence vibrations (3111 and 2932 cm^{-1}), O–H vibrations (3398 cm^{-1}) and the characteristic peak for the C=O group of the DMF molecules (1670 cm^{-1}) (Figure S2). Photoluminescence measurements of **5** reveal a broad excitation peak at $\lambda = 347\text{ nm}$ (detection at 425 nm) and a broad emission peak at $\lambda = 416\text{ nm}$ (excitation at 350 nm).

The compound $[\text{Zn}_3(\text{tdc})_3(\text{DMF})_3] \cdot 0.8\text{DMF} \cdot 1.3\text{H}_2\text{O}$ (**6**) was prepared by further heating of the crystals of **5** (vide infra) at 90°C for one day. Overall, after two days of heating, the shape of the crystalline precipitate was changed to the 3D polyhedrons (Figure S10b). The product was isolated with moderate yield, and its crystal structure and chemical composition were established by a single-crystal X-ray diffraction method and confirmed by elemental, thermogravimetric and IR analysis. The asymmetric unit of the structure **6** contains three zinc(II) cations (Figure S12). Zn(1) has

a distorted octahedral coordination environment consisting of six O atoms of four tdc^{2-} anions and one DMF ligand. One of the COO-groups is coordinated to Zn(1) bidentately with one Zn–O distance being longer than the other one. Zn(2) has a distorted pentagonal pyramidal coordination environment consisting of five O atoms of three tdc^{2-} anions and two DMF ligands. Zn(3) has a distorted octahedral coordination environment of five tdc^{2-} anions, as one of the COO-groups is coordinated to Zn(3) in a bidentate manner. Zn–O distances are in the range 1.9746(14)–2.2615(15) Å. Zn(II) cations are interconnected via bridging carboxylate groups to form trinuclear linear unit $\{\text{Zn}_3(\mu_2\text{-RCOO})_5(\text{dmf})_3(\text{RCOO})_2\}$. These units are further extended through a bridging carboxylate group into polymeric chains in a head-to-tail mode (i.e., Zn(1) of one trinuclear unit is always connected to Zn(2) of another one), running along the *c* axis (Figure 7a). Finally, these chains are interlinked by thiophenedicarboxylate bridges to form a 3D metal-organic framework with narrow triangular channels along the *c* axis (Figure 7b).

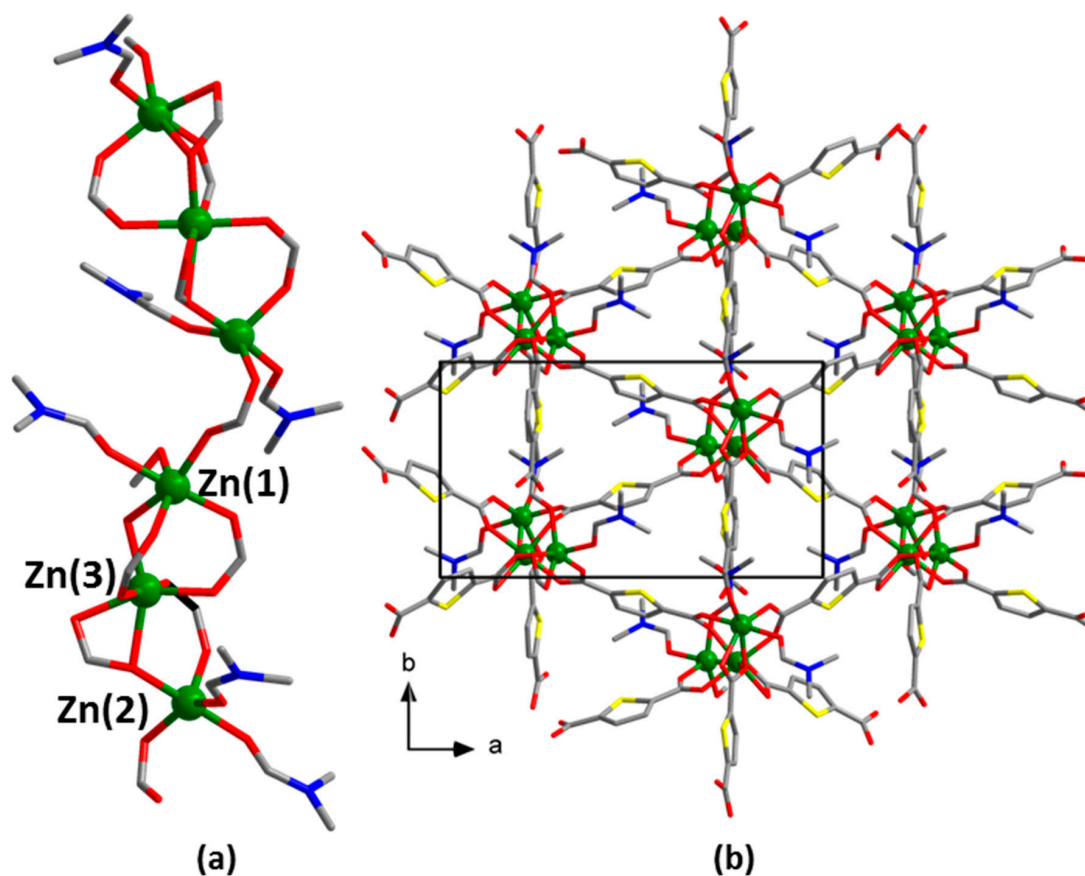


Figure 7. (a) Fragment of a polymeric chain in the structure 6; (b) crystal packing in the structure 6. Hydrogen atoms are omitted. Zn(II) cations are shown with green balls.

The powder X-ray diffraction data support the phase purity of the sample (Figure 5). Microelemental (CHNS) analyses, thermogravimetric analysis and FT-IR spectroscopy confirm the chemical formula of 6 and support the nature of the compound. The TGA of 6 shows a two-step decomposition curve (Figure S13). The first weight loss (22.0 mass. %) at 260 °C corresponds to the elimination of three coordinated DMF molecules. The irreversible thermolysis of the framework 6 starts above 320 °C. The IR spectrum of 6 shows typical stretchings for carboxylate groups (1576 and 1372 cm^{-1}), C–H valence vibrations (3113 and 2932 cm^{-1}), O–H vibrations (3420 cm^{-1}) and the characteristic peak for the C=O group of the DMF molecules (1668 cm^{-1}) (Figure S3). Photoluminescence measurements of 6 reveal a broad excitation peak at $\lambda = 350$ nm (detection at 425 nm) and broad emission peak at $\lambda = 422$ nm (excitation at 350 nm).

4. Discussion

Despite our numerous efforts, the crystalline phases of the coordination polymers **1** and **2** were always contaminated by another crystalline phase of zinc(II) thiophenedicarboxylate, whose structure and properties will be reported elsewhere. The compound **3** was obtained with marginally low yield, rendering impossible a full characterization of the compounds aside from the single-crystal X-ray diffraction and elemental (CHN) analyses. Among all conditions, only the reaction mixture of **4** was modified with the addition of various Na(I) compounds, which expectedly results in the incorporation of Na(I) cations into the coordination structure. Furthermore, the addition of base (NaOH), compared to the neutral salts (e.g., NaBr or NaNO₃), facilitates a deprotonation of the 2,5-thiophenedicarboxylic acid, thus greatly increasing the yield of **4** to a virtually quantitative one. Furthermore, the compounds **5** and **6** were obtained in very similar reaction conditions with the reaction time being the only factor. It indicates that the compound **5**, which crystallizes after one day of heating, is a less thermodynamically stable product than the compound **6**, which is formed after re-crystallization of **5** after another day of heating. The apparently greater stability of the phase **6** could result from an increased density and dimensionality of the metal-organic framework due to “polycondensation” of the isolated trinuclear building units {Zn₃(RCOO)₆}, found in **5**, into infinite chains, featured in **6**. Such an important interplay between the thermodynamics and kinetics of the formation of the crystals of MOFs is rarely reported in such chemistry [24,25].

Three reported compounds (**2**, **5**, **6**) are based solely on trinuclear carboxylate {Zn₃(RCOO)₆} linear building units, sometime referred to as “pin-wheel” complexes. Furthermore, the compound **3** contains these complexes as a part of more complicated pentanuclear motives. The trinuclear linear carboxylate blocks are rather common in zinc-organic frameworks, as well as in other MOFs [26] and often result in layered structures with a trigonal pattern of the 2D grids (**hxl**), as found in the compound **5**. However, other topologies with higher (3D) dimensionalities may also be observed in such MOFs, distorted primitive-cubic (**pcu**), featured in **2**, being a notable example [27]. The formation of terminal dabco molecules in **2** is surprising as this ligand is a very strong donor and tends to coordinate from both nitrogen atoms [28]. The most recent Crystal Structure Database (CSD ver. 5.38, updates May 2017) search reveals only 55 hits (12% out of the total 469 dabco-based coordination complexes) where mono-coordinating dabco ligands have ever been elucidated. The zinc(II)-containing MOF structures **1**, **3** and **4** are rather unique as we fail to find any similar type of networks in the CSD.

The solid-state photoluminescence properties were studied for compounds **4–6** since these were obtainable in bulk amounts. As a reference, the luminescence spectrum of a sodium thiophenedicarboxylate salt Na₂tdc was also recorded. Due to its ionic nature, the corresponding excitation/emission may only result from intraligand $\pi \leftrightarrow \pi^*$ electron transitions of the tdc²⁻ anion. Both the excitation and emission spectra of the coordination polymers **4–6**, as well as Na₂tdc were found to be alike (Figure 8), indicating a similar nature of the luminescence. This is not to be unexpected since zinc(II) cations usually do not interfere with the nature of the ligand-centered electron transitions, not to mention spectroscopically innocent Na(I) ions. In particular, the maxima of the excitation ($\lambda = 375$ nm) and emission ($\lambda = 434$ nm) peaks for **4** coincide with those for the reference compound Na₂tdc, which agrees with the markedly anionic nature of the tdc²⁻ species in the sodium-containing **4**. The peaks of the luminescence spectra for the zinc-based coordination polymers **5** and **6** exhibit a minor shift to higher energies. The recorded maxima for the compound **5** were observed at 347 and 416 nm for the excitation and emission lines, respectively, while for **6**, these were found at 350 and 422 nm. Such hypsochromic shift of the peaks is plausibly related to a lower actual charge on the thiophenedicarboxylate anions in **5** and **6** as a result of a more covalent nature of the Zn–O coordination bonds, compared to mainly ionic Na–O bonds in **4** and Na₂tdc. The measured intensities of the photoluminescence for all compounds were relatively low; however, we were able to determine the quantum yield $\phi = 2\%$ for **6**.

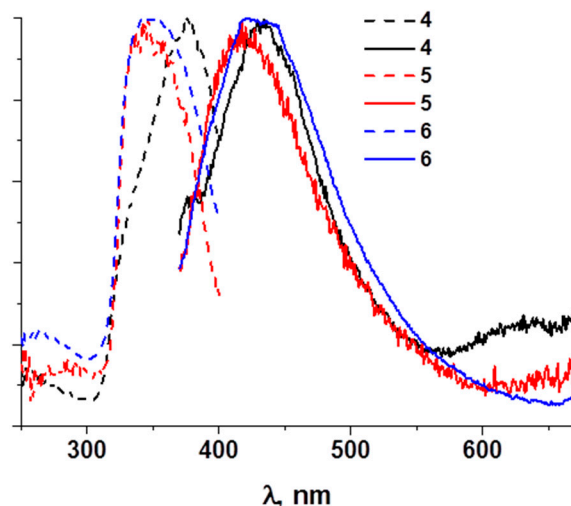


Figure 8. Solid-state luminescence spectra of the compounds 4–6. The emission spectra are shown with solid lines ($\lambda_{\text{ex}} = 350$ nm), and the excitation spectra are shown with dashed lines ($\lambda_{\text{em}} = 425$ nm).

5. Conclusions

In summary, six new metal-organic frameworks based on 2,5-thiophendicarboxylic acid and zinc(II) ions were obtained in a rather narrow range of synthetic conditions. Moreover, a rarely reported kinetic vs. thermodynamic interplay was observed for two particular compounds as a longer reaction time results in a complete re-crystallization of a less stable structure into a new product. Four out of six compounds feature trinuclear linear carboxylate building units $\{\text{Zn}_3(\text{RCOO})_6\}$, which are rather common in MOF chemistry, interconnected into different types of topologies. Interestingly, in one compound, such units were found to be decorated by mono-coordinated dabco ligands. The solid state photoluminescence measurements reveal the influence of the chemical composition on the luminescence properties of the investigated materials as lower energies (longer wavelengths) of the peaks were detected for sodium(I)-containing compounds.

Supplementary Materials: The following are available online at www.mdpi.com/2073-4352/8/1/7, Table S1: Selected bond lengths and angles for **1**; Table S2: Selected bond lengths and angles for **2**; Table S3: Selected bond lengths and angles for **3**; Table S4: Selected bond lengths and angles for **4**; Table S5: Selected bond lengths and angles for **5**; Table S6: Selected bond lengths and angles for **6**; Figure S1: IR spectrum of compound **4**; Figure S2: IR spectrum of compound **5**; Figure S3: IR spectrum of compound **6**; Figure S4: Coordination environment of Zn(II) cation in the structure **1**. Ellipsoids of 50% probability. Hydrogen atoms are omitted. Symmetry codes for related atoms: (i) $\frac{1}{2} - x, \frac{1}{2} - y, z$; (ii) $x, 1 - y, z$; (iii) $\frac{1}{2} - x, \frac{1}{2} + y, z$; (iv) $-x, 1 - y, z$; (v) $1 - x, 1 - y, 1 - z$; Figure S5: Coordination environment of Zn(II) cations in the structure **2**. Ellipsoids of 50% probability. Hydrogen atoms are omitted. Symmetry codes for related atoms: (i) $1 - x, y - \frac{1}{2}, \frac{1}{2} - z$; (ii) $1 - x, 1 - y, -z$; (iii) $x, 3/2 - y, z - \frac{1}{2}$; (iv) $x - 1, y, z$; (v) $2 - x, 1 - y, -z$; Figure S6: Coordination environment of Zn(II) cations in the structure **3**. Ellipsoids of 50% probability. Hydrogen atoms are omitted. Alternative disposition of tdc^{2-} anions is shown by a dashed line. Symmetry codes for related atoms: (i) $-x, 1 - y, 1 - z$; (ii) $\frac{1}{2} - x, \frac{1}{2} - y, 1 - z$; (iii) $\frac{1}{2} + x, y - \frac{1}{2}, z$; (iv) $\frac{1}{2} - x, \frac{1}{2} + y, 3/2 - z$; (v) $\frac{1}{2} - x, \frac{1}{2} + y, \frac{1}{2} - z$; Figure S7: Representation of void space in the structure **3**; Figure S8: Coordination environment of Zn(II) and Na^+ cations in the structure **4**. Ellipsoids of 50% probability. Hydrogen atoms are omitted. Alternative disposition of tdc^{2-} anions and DMF molecules are shown by a dashed line. Symmetry codes for related atoms: (i) $\frac{1}{2} - x, y, z$; (ii) $x, y, 1 + z$; (iii) $x, \frac{1}{2} + y, \frac{1}{2} + z$; (iv) $x, y, z - 1$; (v) $x, \frac{1}{2} + y, z - \frac{1}{2}$; (vi) $\frac{1}{2} - x, y, z - 1$; (vii) $1 - x, 1 - y, z$; Figure S9: TG curve of compound **4**; Figure S10. (a) Crystals of **5**; (b) crystals of **6**; Figure S10. Coordination environment of Zn(II) cations in the structure **5**. Ellipsoids of 50% probability. Hydrogen atoms are omitted. Symmetry codes for related atoms: (i) $3/2 - x, \frac{1}{2} + y, \frac{1}{2} - z$; (ii) $\frac{1}{2} - x, \frac{1}{2} - y, \frac{1}{2} - z$; (iii) $x, 1 + y, z$; Figure S11: TG curve of compound **5**; Figure S12: Coordination environment of Zn(II) cations in the structure **6**. Ellipsoids of 50% probability. Hydrogen atoms are omitted. Symmetry codes for related atoms: (i) $1 - x, y - \frac{1}{2}, \frac{1}{2} - z$; (ii) $-x, \frac{1}{2} + y, \frac{1}{2} - z$; (iii) $x, \frac{1}{2} - y, z - \frac{1}{2}$; (iv) $x, 3/2 - y, z - \frac{1}{2}$; Figure S13: TG curve of compound **6**. Crystallographic data for the structural analysis have been deposited with the Cambridge Crystallographic Data Centre, CCDC Nos. 1586559–1586564. Copies of the data

can be obtained free of charge from the Cambridge Crystallographic Data Centre, 12 Union Road, Cambridge CB2 1EZ, U.K. (fax: +44-1223-336-033; e-mail: deposit@ccdc.cam.ac.uk).

Acknowledgments: The work was supported by the Russian Science Foundation (Project No. 14-23-00013). The authors are grateful to Alexey Ryadun for luminescence measurements.

Author Contributions: Danil Dybtsev and Vladimir Fedin conceived of and designed the experiments. Anna Lysova carried out the synthesis. Denis Samsonenko performed the X-ray structure determination and analyzed the results.

Conflicts of Interest: The authors declare no conflict of interest. The founding sponsors had no role in the design of the study; in the collection, analyses or interpretation of data; in the writing of the manuscript; nor in the decision to publish the results.

References

1. Allendorf, M.D.; Bauer, C.A.; Bhakta, R.K.; Houka, R.J.T. Luminescent metal-organic frameworks. *Chem. Soc. Rev.* **2009**, *38*, 1330–1352. [[CrossRef](#)] [[PubMed](#)]
2. Zhou, W.; Wu, Y.-P.; Zhou, Z.-H.; Qin, Z.-S.; Ye, X.; Tian, F.-Y.; Li, D.-S. Construction of a series of lanthanide metal-organic frameworks (Ln-MOFs) based on a new symmetrical penta-aromatic carboxylate strut: Structure, luminescent and magnetic properties. *Inorg. Chim. Acta* **2016**, *453*, 757–763. [[CrossRef](#)]
3. Takashima, Y.; Martínez, V.M.; Furukawa, S.; Kondo, M.; Shimomura, S.; Uehara, H.; Nakahama, M.; Sugimoto, K.; Kitagawa, S. Molecular decoding using luminescence from an entangled porous framework. *Nat. Commun.* **2011**, *2*, 168. [[CrossRef](#)] [[PubMed](#)]
4. Hu, Z.; Deibert, B.J.; Li, J. Luminescent metal-organic frameworks for chemical sensing and explosive detection. *Chem. Soc. Rev.* **2014**, *43*, 5815–5840. [[CrossRef](#)] [[PubMed](#)]
5. Müller-Buschbaum, K.; Beuerle, F.; Feldmann, C. MOF based luminescence tuning and chemical/physical sensing. *Micropor. Mesopor. Mater.* **2015**, *216*, 171–199. [[CrossRef](#)]
6. Duan, J.; Jin, W.; Kitagawa, S. Water-resistant porous coordination polymers for gas separation. *Coord. Chem. Rev.* **2017**, *332*, 48–74. [[CrossRef](#)]
7. Agarwal, R.A.; Gupta, N.K. CO₂ sorption behavior of imidazole, benzimidazole and benzoic acid based coordination polymers. *Coord. Chem. Rev.* **2017**, *332*, 100–121. [[CrossRef](#)]
8. Zhai, Q.-G.; Bu, X.; Zhao, X.; Li, D.-Zh.; Feng, P. Pore space partition in metal-organic frameworks. *Acc. Chem. Rev.* **2017**, *50*, 407–417. [[CrossRef](#)] [[PubMed](#)]
9. Aquirre-Díaz, L.M.; Reinares-Fisac, D.; Iglesias, M.; Gutiérrez-Puebla, E.; Gándara, F.; Snejko, N.; Ángeles Monge, M. Group 13th metal-organic frameworks and their role in heterogeneous catalysis. *Coord. Chem. Rev.* **2017**, *335*, 1–27. [[CrossRef](#)]
10. Liu, J.; Chen, L.; Cui, H.; Zhang, J.; Zhang, L.; Su, C.-Y. Applications of metal-organic frameworks in heterogeneous supramolecular catalysis. *Chem. Soc. Rev.* **2014**, *43*, 6011–6061. [[CrossRef](#)] [[PubMed](#)]
11. Chughtai, A.H.; Ahmad, N.; Younus, H.A.; Laypkov, A.; Verpoort, F. Metal-organic frameworks: Versatile heterogeneous catalysts for efficient catalytic organic transformations. *Chem. Soc. Rev.* **2015**, *44*, 6804–6849. [[CrossRef](#)] [[PubMed](#)]
12. Wuttke, S.; Lismont, M.; Escudero, A.; Rungtaweevoranit, B.; Parak, W.J. Positioning metal-organic framework nanoparticles within the context of drug delivery—A comparison with mesoporous silica nanoparticles and dendrimers. *Biomaterials* **2017**, *123*, 172–183. [[CrossRef](#)] [[PubMed](#)]
13. An, J.; Geib, S.J.; Rosi, N.L. Cation-triggered drug release from a porous zinc-adeninate metal-organic framework. *J. Am. Chem. Soc.* **2009**, *131*, 8376–8377. [[CrossRef](#)] [[PubMed](#)]
14. Wuttke, S.; Zimpel, A.; Bein, T.; Braig, S.; Stoiber, K.; Vollmar, A.; Müller, D.; Haastert-Talini, K.; Schaeske, J.; Stiesch, M.; et al. Validating metal-organic framework nanoparticles for their nanosafety in diverse biomedical applications. *Adv. Healthc. Mater.* **2017**, *6*, 1600818. [[CrossRef](#)] [[PubMed](#)]
15. Osborn Popp, T.M.; Yaghi, O.M. Sequence-Dependent Materials. *Acc. Chem. Res.* **2017**, *50*, 532–534. [[CrossRef](#)] [[PubMed](#)]
16. Deng, H.; Doonan, C.J.; Furukawa, H.; Ferreira, R.B.; Towne, J.; Knobler, C.B.; Wang, B.; Yaghi, O.M. Multiple functional groups of varying ratios in metal-organic frameworks. *Science*. **2010**, *327*, 846–850. [[CrossRef](#)] [[PubMed](#)]
17. Furukawa, H.; Müller, U.; Yaghi, O.M. “Heterogeneity within order” in metal-organic frameworks. *Angew. Chem. Int. Ed.* **2015**, *54*, 3417–3430. [[CrossRef](#)] [[PubMed](#)]

18. Kleist, W.; Jutz, F.; Maciejewski, M.; Baiker, A. Mixed-Linker metal-organic frameworks as catalysts for the synthesis of propylene carbonate from propylene oxide and CO₂. *Eur. J. Inorg. Chem.* **2009**, *2009*, 3552–3561. [[CrossRef](#)]
19. Stock, N.; Biswas, S. Synthesis of metal-organic frameworks (MOFs): Routes to various MOF topologies, morphologies, and composites. *Chem. Rev.* **2012**, *112*, 933–969. [[CrossRef](#)] [[PubMed](#)]
20. *CrysAlisPro 1.171.38.41*, Rigaku Oxford Diffraction: The Woodlands, TX, USA, 2015.
21. Sheldrick, G.M. *SHELXT* - integrated space-group and crystal-structure determination. *Acta Crystallogr. A* **2015**, *A71*, 3–8. [[CrossRef](#)] [[PubMed](#)]
22. Sheldrick, G.M. Crystal structure refinement with *SHELXL*. *Acta Crystallogr. C* **2015**, *C71*, 3–8. [[CrossRef](#)] [[PubMed](#)]
23. Spek, A.L. *PLATON SQUEEZE*: A tool for the calculation of the disordered solvent contribution to the calculated structure factors. *Acta Crystallogr. C* **2015**, *C71*, 9–18. [[CrossRef](#)] [[PubMed](#)]
24. Wu, Y.; Henke, S.; Kieslich, G.; Schwedler, J.; Yang, M.; Fraser, D.A.X.; O'Hare, D. Time-resolved in situ X-ray diffraction relates metal-dependent metal-organic framework formation. *Angew. Chem. Int. Ed.* **2016**, *55*, 1–5. [[CrossRef](#)] [[PubMed](#)]
25. Marti-Rujas, J.; Kawano, M. Kinetic products in coordination networks: Ab initio X-ray powder diffraction analysis. *Acc. Chem. Res.* **2013**, *46*, 493–505. [[CrossRef](#)] [[PubMed](#)]
26. Tranchemontagne, D.J.; Mendoza-Cortés, J.L.; O'Keeffe, M.; Yaghi, O.M. Secondary building units, nets and bonding in the chemistry of metal-organic frameworks. *Chem. Soc. Rev.* **2009**, *38*, 1257–1283. [[CrossRef](#)] [[PubMed](#)]
27. Dincă, M.; Long, J.R. Strong H₂ binding and selective gas adsorption within the microporous coordination solid Mg₃(O₂C-C₁₀H₆-CO₂)₃. *J. Am. Chem. Soc.* **2005**, *127*, 9376–9377. [[CrossRef](#)] [[PubMed](#)]
28. Sapchenko, S.; Dybtsev, D.; Fedin, V. Cage amines in the metal-organic frameworks chemistry. *Pure Appl. Chem.* **2017**, *89*, 1049–1064. [[CrossRef](#)]



© 2017 by the authors. Licensee MDPI, Basel, Switzerland. This article is an open access article distributed under the terms and conditions of the Creative Commons Attribution (CC BY) license (<http://creativecommons.org/licenses/by/4.0/>).